EXTREMAL CONTROL FOR PHOTOVOLTAIC PANELS

Prof. Genevieve DAPHIN TANGUY,
prof. Dumitru POPESCU, ing. Crina TOROUS, student Chloe LOURDAIS

Rezumat. Lucrarea propune o procedura de control extremal folosind un controller de tip polinomial pentru utilizarea eficienta a panourilor fotovoltaice. Deasemenea, a fost dezvoltata si o structura de testare a sistemelor de urmărire solara prin intermediul unei arhitecturi Hardware In the Loop. Metode de optimizare eficiente bazate pe tehnici de gradient au fost implementate pentru a determina parametrii panoului cat si pentru a calcula punctul de maximă putere generată (MPPT). Un controler de tip RST a fost dezvoltat pentru a urmări mişcarea soarelui spre atingerea maximului de putere posibil. După o analiza de robustete, comanda (nominala) proiectata este îmbunătățită, în vederea implementarii pe sisteme care pilotează sisteme fotovoltaice. Configurația Hardware In the Loop permite dezvoltarea unei platforme de test şi dezvoltare care poate fi folosită la aducerea de ameliorări în designul actual şi, de asemenea, la testarea a diferiți algoritmi de control. Performantele sistemului robust pentru un panou cu orientare valabilă, sunt validate in simulare folosind mediul de programare MATLAB/SIMULINK si produsul software dedicat WinPim & WinReg.

Abstract. In this paper a methodology for extremal control of photovoltaic panels has been designed through the use of an embedded polynomial controller using robust approaches and algorithms. Also, a framework for testing solar trackers in a hard ware in the loop (HIL) configuration has been established. Efficient gradient based optimization methods were put in place in order to determine the parameters of the employed photovoltaic panel, as well as for computing the Maximum Power Point (MPP). Further a numerical RST controller has been computed in order to allow the panel to follow the movement of the sun to obtain a maximum energetic efficiency. A robustness analysis and correction procedure has been done on the RST polynomial algorithm. The hardware in the loop configuration allows for the development of a test and development platform which can be used for bringing improvements to the current design and also test different control approaches. For this, a microcontroller based solution was chosen. The achieved performances of the closed loop photovoltaic panel (PP) system are validated in simulation using the MATLAB / SIMULINK environment and the WinPim & WinReg dedicated software. As it will be seen further in this paper, the extremal control of this design resides in a sequential set of computations used for obtaining the new Maximum Power Point at each change in the system.

Keywords: identification, optimal criterion, adaptive and robust control, industrial process, simulation results

1. Introduction

Photovoltaic panels are an important source of renewable energy [1]. Because of the low physical performances of a photovoltaic cell numerous optimization techniques have been implemented to overcome this. Our solution is to use an

optimal algorithm for computing the Maximum Power Point and designing a robust RST controller which rotates the photovoltaic panel in order to follow the sun's movement.

The rotation of the panel can be done on two axes. In this paper the movement of the panel on a vertical axis is considered fixed and the positioning of the panel towards the sun is controlled.

The extremal control in this paper consists of computing, in real time, the Maximum Power Point, using optimal algorithms, such as the gradient Cauchy algorithm and the Coggin's algorithm and using a robust RST controller to rotate the panel to face the sun directly.

2. Photovoltaic panel – Modelling and characteristics

2.1. Two diodes model

The functioning of a PN junction allows achieving an equivalent circuit model of a photovoltaic cell called the ideal model. This model is a current source connected in parallel to a diode. This is the simplest model to represent a photovoltaic cell; it has the advantage of having a reduced number of parameters (three parameters) required for the simulation of the characteristic curves I-V and P-V. However it exhibits serious deficiencies when subjected to temperature and irradiance variations. An improvement of this model is done by the inclusion of one series resistance R_s and one shunt resistance R_p.

This new model, called one diode model, is the most popular approach: it has a low number of unknown parameters (five parameters) and is more accurate than the ideal model, especially because it takes more account of the change in the environment. Furthermore, the most precise model, which will be used in this article, is the two diodes model, shown in Fig. 1 [4].
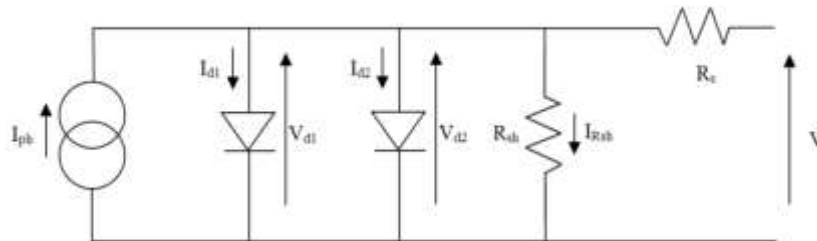

Fig. 1. Photovoltaic panel – Two diodes model

The output current of the photovoltaic cell can be written as:

$$I = I_{ph} - I_{01}\left[\exp\left(\frac{V + IR_s}{a_1 V_T}\right) - 1\right] - I_{02}\left[\exp\left(\frac{V + IR_s}{a_2 V_T}\right) - 1\right] - \frac{V + IR_s}{R_p} \tag{1}$$

Table 1. Parameters of the characteristic equation (1)

Notation	Definition
I	Output current of the PV cell
V	Output voltage of the PV cell
I_{ph}	Photogenerated current by the incidence of light
I_{01}, I_{02}	Reverse saturation currents of the two diodes
a_1, a_2	Ideality factors of the two diodes
$V_T = N_s . k_b . T / q$	Thermodynamic potential: - Ns is the number of cells in series - q is the electron charge ($1.60217646.10^{-19}$ C), - k is the Boltzmann constant ($1.3806503.10^{-23}$ J/K).
R_s	Series resistance
R_p	Shunt resistance

Several parallel and series cells compose a photovoltaic module. N_p (generally $N_p=1$) gives the number of cells connected in parallel and N_s the number of series cells (N_s varies between 34 and 56 cells). In the cases where $N_p=1$, the characteristic equation (1) is the same but the thermodynamic potential V_T depends on N_s [3].

2.2. Parameters identification

The equation (1) is an implicit equation where *I* and *V* can be solved thanks to the method of Newton-Raphson or analytically. This model has seven parameters: I_{ph}, I_{01}, I_{02}, a_1, a_2, R_s and R_p and the objective of this part is to determine these unknown parameters in order to compute the *I-V* and *P-V* characteristic curves. The value of I_{ph} is calculated from the irradiance and temperature measurements and the values of I_{01}, I_{02}, R_s, and R_p can be calculated from the datasheets of the photovoltaic panel. Indeed, each photovoltaic module has specific characteristics given by the datasheet information provided by the manufacturer. The datasheet of the photovoltaic panel used in this article: "Ameresco Solar 30J" is:

Table 2. Photovoltaic panel Ameresco Solar 30J - Datasheet

PV parameters: Ameresco Solar 30J		Values
T_{STC}	Temperature at Standard Test Conditions	25°C
G_{STC}	Irradiance at Standard Test Conditions	1000 W.m^{-2}
V_{oc_STC}	Open circuit voltage	22.1 V
I_{sc_STC}	Short circuit current	1.74 A
P_{mp_STC}	Maximum power	30 W
V_{mp_STC}	Voltage at P$_{mp\_STC}$	17.9 V
I_{mp_STC}	Current at P$_{mp\_STC}$	1.68 A
K_i	Temperature coefficient of I$_{sc\_STC}$	0.105 %/°C

K_v	Temperature coefficient of V_{oc_STC}	-0.360 %/°C
N_s	Number of cells in series	36

Determination of the photogenerated current I_{ph}:

The equation for the current generated by the incidence of light I_{ph}, as a function of temperature and irradiance, can be given by:

$$I_{ph} = \left(I_{ph\_STC} + K_i \mathrm{D}T\right)\frac{G}{G_{STC}} \tag{2}$$

Where G is the surface irradiance of the cell and $\Delta T = T_{STC} - T$ is the difference between the external temperature and the temperature at Standard Test Conditions. The other values are available from the datasheet (see Table 2).

Determination of the two diodes parameters I_{01}, I_{02}, a_1, and a_2:

First, the two diodes saturation current equation, which considers the temperature variation, is given by:

$$I_{01} = I_{02} = \frac{I_{SC\_STC} + K_i \mathrm{D}T}{\exp\left(\dfrac{V_{oc\_STC} + K_v \mathrm{D}T}{\left(\dfrac{a_1 + a_2}{p}\right)V_T}\right) - 1} \tag{3}$$

Diode ideality factors a_1 and a_2 represent, respectively, the diffusion and recombination current component. Several researchers show that the diffusion current a_1 must be unity and the value of a_2 is flexible. It is found that the best match between the proposed model and practical *I-V* curve is observed when $(a_1+a_2)/p=1$ and $p \geq 2,2$.

Here, we have found that the best value of a_1 and a_2 are respectively 1 and 1.2. To conclude, the expression for the diode saturation current of the two diodes I_{01} and I_{02} is:

$$I_{01} = I_{02} = \frac{I_{SC\_STC} + K_i \mathrm{D}T}{\exp\left(\dfrac{V_{oc\_STC} + K_v \mathrm{D}T}{V_T}\right) - 1} \tag{4}$$

Determination of R_p and R_s values:

The series resistance, in the figure (1), called R_s, models the resistance contained in the semiconductor and the shunt resistance, named R_p in the figure, models the current leakage through a resistive branch which is parallel to the generator and to the two diodes.

These losses are less important than those represented by the resistance R_s; so the value of the resistance R_s is much lower than the value of R_p.

The values of the resistors R_s and R_p are obtained by iteration and calculated simultaneously. According to the characteristic equation (1), at maximum power point, R_p can be expressed in terms of R_s as follows:

$$R_p = \frac{V_{mp\_STC} + I_{mp\_STC}.R_s}{I_{ph} - I_{01}\left[\exp\left(\frac{V_{mp\_STC} + I_{mp\_STC}.R_s}{a_1 V_T}\right) - 1\right] - I_{02}\left[\exp\left(\frac{V_{mp\_STC} + I_{mp\_STC}.R_s}{a_2 V_T}\right) - 1\right] - \frac{P_{mp\_E}}{V_{mp\_STC}}} \tag{5}$$

The voltage V_{mp_STC}, the current I_{mp_STC}, and the power P_{mp_STC} are at maximum power point. These data are supplied by the manufacturer datasheets.

The idea of the following algorithm is, by iteratively increasing the value of R_s while simultaneously calculating the R_p value, to compare the value of the calculated maximum power point P_{mp_C}, with the value of experimental maximum power $P_{mp\_E}=P_{mp\_STC}$, given by the manufacturer's datasheets, in order to have the smallest difference.

In this paper we use Newton Raphson's method to solve the equation (6) and find the value of I ($0 \leq I \leq I_{sc\_STC}$) for different values of V ($0 \leq V \leq V_{oc\_STC}$):

$$f(I) = I - I_{ph} + I_{01}\left[\exp\left(\frac{V + IR_s}{a_1 V_T}\right) - 1\right] + I_{02}\left[\exp\left(\frac{V + IR_s}{a_2 V_T}\right) - 1\right] + \frac{V + IR_s}{R_p} = 0 \tag{6}$$

This method is described by this expression:

$$I_{n+1} = I_n - \frac{f(I_n)}{f'(I_n)} \tag{1}$$

With the set of data of *I* and *V*, it is possible to calculate de power *P* and the maximum power P_{mp_C} and apply the following algorithm:
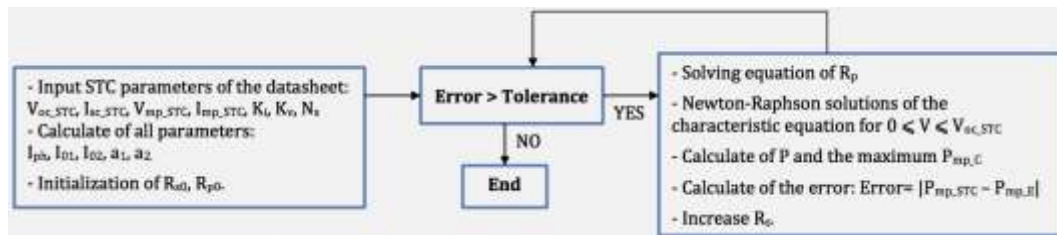

Fig. 2. Algorithm for the determination of Rs and Rp using the Newton-Raphson method.

Table 3. Results of parameters calculation

$I_{01}=I_{02}$	I_{ph}	a_1	a_2	R_s	R_p
$7.31.10^{-11}$ A	1.74 A	1	1,2	0.892 Ω	529.657 Ω

With these values of resistors R_s and R_p and the simulation given by the resolution of the characteristic equation (1), we find a voltage at maximum power point of $V_{mp\_C} = 17{,}89$ V ($V_{mp\_STC} = 17{,}9$ V) and a power at the maximum power point of $P_{mp\_C} = 28{,}88$ W ($P_{mp\_STC} = 30$ W).

These results confirm the model because the results given by the simulations are close to the experimental values.

2.3. Characteristics

These results allow plotting the characteristic curves *I-V* and *P-V* by using the Newton-Raphson method.

In the figures that follow, it can be noticed that the model offers a good approximation of the real one.

We can note that there is a special point where the photovoltaic panel provides the maximum power. The objective of this article is to control a photovoltaic panel in order for it to work at the maximum power point.
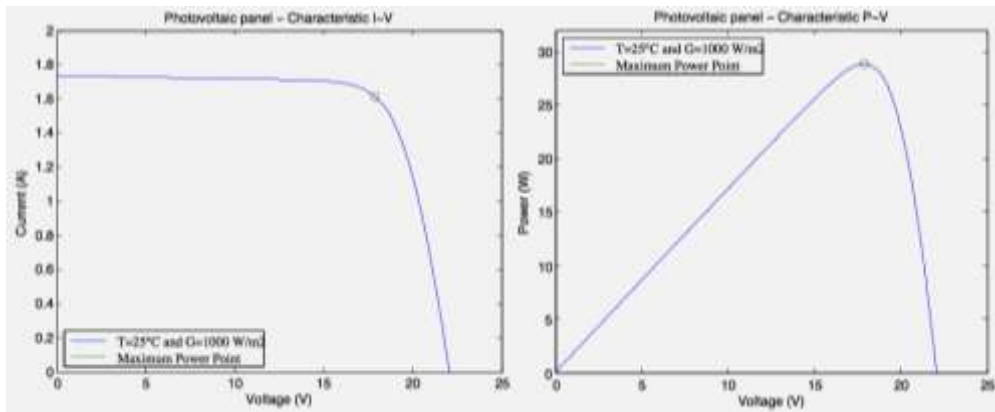

Fig. 3. Simulation of the characteristic *I-V* and *P-V* of the Ameresco Solar photovoltaic panel.
a. Characteristic *I-V*;   **b.** Characteristic *P-V*.

3.   Maximum power point tracking

The objective is to control the maximum power of a photovoltaic panel with a DC motor that allows the solar panel to follow the direction of sunlight.

First, an algorithm compute the maximum power point, here we use the gradient algorithm.

Secondly, a RST controller control the system composed of a DC motor and the photovoltaic panel in order to the system works at the power imposed by a power generator, liaising between the numerical power given by the algorithm and the physical complete system {DC motor + Photovoltaic panel}.XII
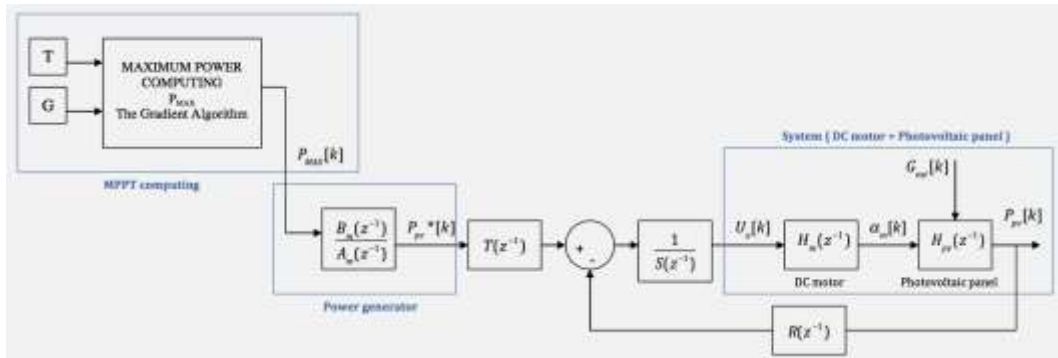
Fig. 4. Diagram of the maximum power point tracking and control.

3.1. The gradient algorithm for computing the MPP

In order to benefit of the maximum power of a photovoltaic panel a MPPT control algorithm will be used. The most popular and the simplest algorithm is Perturb and Observe (P&O). Currently, many applications in industry use this algorithm.

In this application, we have chosen the gradient algorithm for its robustness and high speed of convergence. The method is applied at the power $P(I,V)$ as a function of the current I and the voltage V. The parameters are: the starting point (I_0,V_0), the direction λ and the precision ε. The next step involves evaluating the gradient of the function P and moving in this direction in order to be close to the maximum power point. The algorithm stops when the gradient becomes too small compared to the precision, which means that the point x_k is near the maximum power point with the precision ε [2].
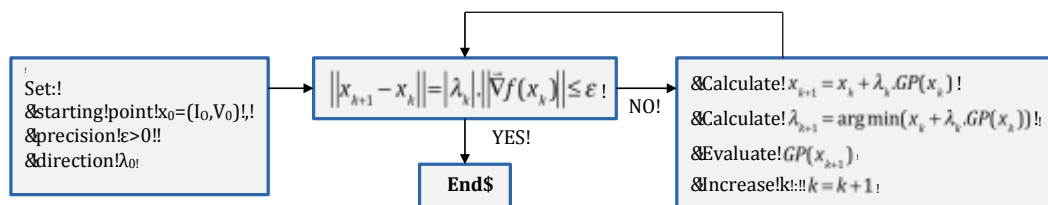

Fig. 5. The gradient algorithm.

Table 4. Results obtained by the gradient algorithm for computing the maximum power point

I_0	V_0	ε	λ_0	V_{mp}	I_{mp}	$P_{mp}=I_{mp}.V_{mp}$
0,5 A	0,4 V	0,0001	0,5	31,25 V	0,62 A	19,32 W

3.2. System { DC motor + Photovoltaic panel } dynamic models

The complete system consists of photovoltaic modules, an electric DC motor, a sensor for measuring the voltage and the current at the terminal of the PV panel.
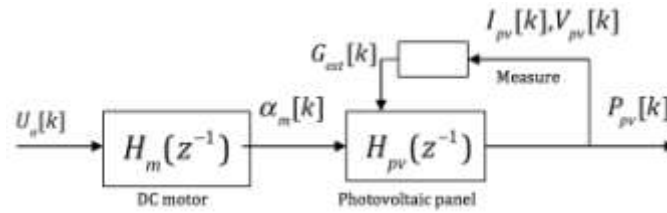
Fig. 6. Block diagram of the system{ DC motor + the photovoltaic panel }.
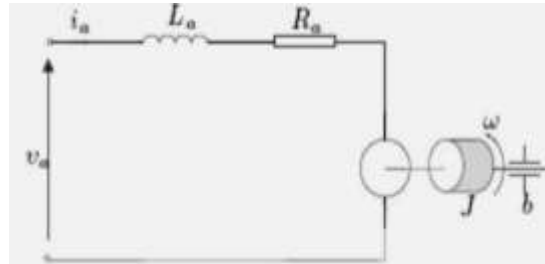
DC motor dynamic model:

Fig. 7. Electric block diagram of the DC motor.

The dynamic of the DC motor may be expressed by the following equation [6]. The first one comes from the Kirchhoff laws and the second one from the angular momentum theorem:

$$u_a(t) = u_{R_a}(t) + u_{L_a}(t) + e_a(t) = R_a.i_a(t) + L_a.\frac{di_a(t)}{dt} + e_a \tag{8}$$

$$J.\frac{dW(t)}{dt} = C_m(t) + C_b(t) = K_c.i_a(t) - b.W(t) \tag{9}$$

Table 5. Parameters of the characteristic equation (1)

Motor parameters		Values
U_a	Armature voltage	V
I_a	Armature current	A
ω_m	Speed of the rotor	$rad.s^{-1}$
R_a	Motor resistance	$1,45\Omega$
L_a	Motor inductance	$15,5.\,10^{-3}\,H$
J	Motor inertia	$0,48kg.m^2$
$e_a(t)=K_e.\omega_m(t)$	Back EMF of the motor	V
$C_m(t)=K_c.i_a(t)$	Motor torque	N.m
$C_b(t)=-b.\omega_m(t)$	Friction torque	N.m
K_c	Motor torque constant	$0,1V.rad^{-1}.s^{-1}$
K_e	Motor voltage constant	$0,1V.rad^{-1}.s^{-1}$
b	Friction coefficient	$0,2m.N.rad^{-1}.s$

The relation between the panel positioning angle and the speed of the rotor is:

$$W(s) = s.a_m(s) \tag{10}$$

Using Laplace Transforms, the above equations can be expressed in terms of s.

$$H_m(s) = \frac{a_m(s)}{U_a(s)} = \frac{1}{s} \cdot \frac{K_e}{(L_a J).s^2 + (R_a J + L_a b).s + (R_a b + K_e^{\ 2})} \tag{11}$$

Photovoltaic panel dynamic model:

The power on a photovoltaic module depends not only on the power contained in the sunlight, but also on the angle between the module and the ray of sunlight. When the surface of the panel and the sunlight are perpendicular to each other the photovoltaic module works at the maximum power point. Indeed, the ray of sunlight with an angle of incidence of 90° tends to be absorbed, while lower angles tend to be reflected. The solar radiation absorbed by the photovoltaic module (G_m) is the component of the incident solar radiation (G_{ext}), which is perpendicular to the module surface [5]. The angle of incidence (α_m) is the angle between the tilted module surface and the external ray of sunlight. Consequently, the expression between these parameters is:

$$G_m = G_{ext}.\sin(a_m) \tag{12}$$

The role of the motor is the photovoltaic panel that follows the solar radiation. Consequently the angle α_m stays very small and we can approximate the function "sin" around the value of zero, see equation (13). We suppose that this approximation is correct for $-15° \leq \alpha_m \leq 15°$. For the start of the experience, we consider that we launch the panel approximately perpendicular to the sunlight because we can know the position of the sunlight.

$$G_m = G_{ext}.a_m \tag{13}$$

Thus, the power delivered by a solar panel positioned at irradiation G_{ext}, which has a component perpendicular to the panel, called G_m, is equal to the maximum power that it could deliver if it was placed at irradiation G_m: $P_{pv\_Gext} = P_{pv\_MAX\_Gm}$.

Besides, the power at maximum power point can be written as the multiplication of the current I_{mp_STC} and the voltage V_{mp_STC}. By using the characteristic equation (1) at the maximum power point: $I = I_{mp\_STC}$ and $V = V_{mp\_STC}$, only the term I_{ph} depends on the radiation G and we have:

$$\frac{dP_{pv\_MAX}}{dG_m} = V_{mp\_STC}.\frac{1}{G_{STC}}.\left(K_i DT + I_{sc\_STC}\right) = K_{pv} \tag{14}$$

The value of K_i is very small and we can neglect the term in K_i, so the derivation of the power at the maximum power point P_{pv_MAX}, compared to the irradiance G_m

is a constant term and the power at maximum point and the external radiation are proportional.

$$P_{pv\_G_{ext}} = P_{pv\_MAX\_G_m} = K_{pv}.G_m = K_{pv}.G_{ext}.a_m \tag{15}$$

To conclude, by using this equation, the transfer function of the solar panel is:

$$H_{pv}(s) = \frac{P_{pv}(s)}{a_m(s)} = K_{pv}.G_{ext} \tag{16}$$

By using a voltmeter and a ammeter to measure the terminal voltage and the current of the photovoltaic panel, it is possible to determine the value of the external radiation with of the following formula, determined by (1) and (2):

$$G_{ext} = \frac{G_{STC}}{I_{sc\_STC}}.\left[I_{pv} + I_{01}.\left(\exp\left(\frac{V_{pv} + I_{pv}R_s}{a_1 V_T} \right) \right) + I_{02}.\left(\exp\left(\frac{V_{pv} + I_{pv}R_s}{a_2 V_T} \right) \right) + \frac{V_{pv} + I_{pv}R_s}{R_p} \right] \tag{17}$$

3.3. Conclusion

To conclude, the transfer function of the photovoltaic and motor system becomes:

$$H(s) = K_{pv}.G_{ext} \frac{K_m}{a_m s^3 + b_m s^2 + c_m s} \tag{18}$$

Where the parameters a_1, a_2, a_3, b_1, b_2 and b_3 depend only on the parameters of the DC motor. The calculus leads to:

$$H(s) = K_{pv}.G_{ext}.\frac{1,000.10^{-1}}{7,440.10^{-3}.s^3 + 6,991.10^{-1}.s^2 + 3,000.10^{-1}.s} \tag{19}$$

By discretizing the continuous model of the system, with a sampling period $T_r = 0,05$s, we have obtained the discrete model of the system, as follows:

$$H(z^{-1}) = \frac{B(z^{-1})}{A(z^{-1})} = K_{pv}.G_{ext}.\frac{B'(z^{-1})}{A'(z^{-1})} \tag{20}$$

Where the function $B'(z^{-1})/A'(z^{-1})$ represent the discrete model of the DC motor. The numerical application gives:

$$\begin{cases} A'(z^{-1}) = 1 - 1,958.z^{-1} + 9,580.10^{-1}.z^{-2} - 8,301.10^{-5}.z^{-3} \\ B'(z^{-1}) = 5,737.10^{-4}.z^{-1} + 8,169.10^{-4}.z^{-2} + 1,573.10^{-5}z^{-3} \end{cases} \tag{21}$$

The variation of the irradiance G_{ext} is low compared to the dynamic of the DC motor. Only the DC motor imposes the dynamics of the system and we consider that the term $G_{ext}.K_{pv}$ is a multiplicative constant. We can conduct the analysis on polynomials $A'(z^{-1})$ and $B'(z^{-1})$.

3.4. Power generator

For computing the A_m and B_m polynomials, we need to impose the pair (ζ_n, ω_{0n}) in order to follow the tracking performances desired. We have imposed $\zeta_n = 0.9$ and $\omega_{0n} = 2.0$ rad.s^{-1}. By discretization, we have obtained:

$$\frac{B_m(z^{-1})}{A_m(z^{-1})} = \frac{0,004709 + 0,004435.z^{-2}}{1 - 1,826126.z^{-1} + 0,835270.z^{-2}} \tag{22}$$

3.5. Digital RST controller design

For the discrete model $A'(z^{-1})/B'(z^{-1})$, a RST controller was designed to achieve distinct performances in tracking and regulation. Controller polynomials $R(z^{-1})$ and $S(z^{-1})$ determine the regulation performances and the polynomial $T(z^{-1})$ involves the performance in tracking [7]. The sample time is also of 0.05 seconds.

The desired poles introduced by the polynomial $P(z^{-1})$, which is the characteristic polynomial of the system, specify the performance of the closed loop system [8].

$$P(z^{-1}) = A'(z^{-1}).S'(z^{-1}) + B'(z^{-1}).R'(z^{-1}) \tag{23}$$

We desire a response of second order for the polynomial P and we have allocated the dominant poles given by $\zeta = 0.9$ and $\omega_0 = 2.5$ rad·s^{-1}. By discretization we can determine the characteristic polynomial $P(z^{-1})$:

$$P(z^{-1}) = 1 - 1,784542.z^{-1} + 0,798516.z^{-2} \tag{24}$$

As a result, the calculation of controller parameters $R'(z^{-1})$ and $S'(z^{-1})$ involves the resolution of the Bézout equation represented by (23), and $T'(z^{-1})$ must be chosen to ensure a static gain between $P_{pv}*[k]$ and $P_{pv}[k]$:

$$T(z^{-1}) = \begin{cases} G = \dfrac{1}{B(1)}, B(1) \neq 0 \\ G = 1 \end{cases} .P(z^{-1}) \tag{25}$$

The following RST controller was obtained by using WinReg, a software tool for automatic control:

$$\begin{cases} R'(z^{-1}) = 590,229758 - 555,672495.z^{-1} + 5,130326.z^{-2} \\ S'(z^{-1}) = 1 + 0,203458.z^{-1} + 0,040261.z^{-2} \\ T'(z^{-1}) = 2840,102244 - 5068,281738.z^{-1} + 2267,867083.z^{-2} \end{cases} \tag{26}$$

For the complete system DC motor and photovoltaic panel, the polynomials R, S and T depend on the polynomials R', S' and T' and the expressions are:

$$R(z^{-1}) = \frac{1}{K_{pv}G_{ext}}R'(z^{-1}), \qquad S(z^{-1}) = S'(z^{-1}), \qquad T(z^{-1}) = \frac{1}{K_{pv}G_{ext}}T'(z^{-1}) \qquad (27)$$

The following Matlab-Simulink diagram block (see Fig. 8) represents the maximum power point tracking (the gradient algorithm) and the control of the system by the previous RST controller, and the figure 9, the response of the complete system. We have inserted a step disturbance at $T = 6$ sec, in order to observe the regulation performance. The RST controller achieves performances in tracking and regulation.
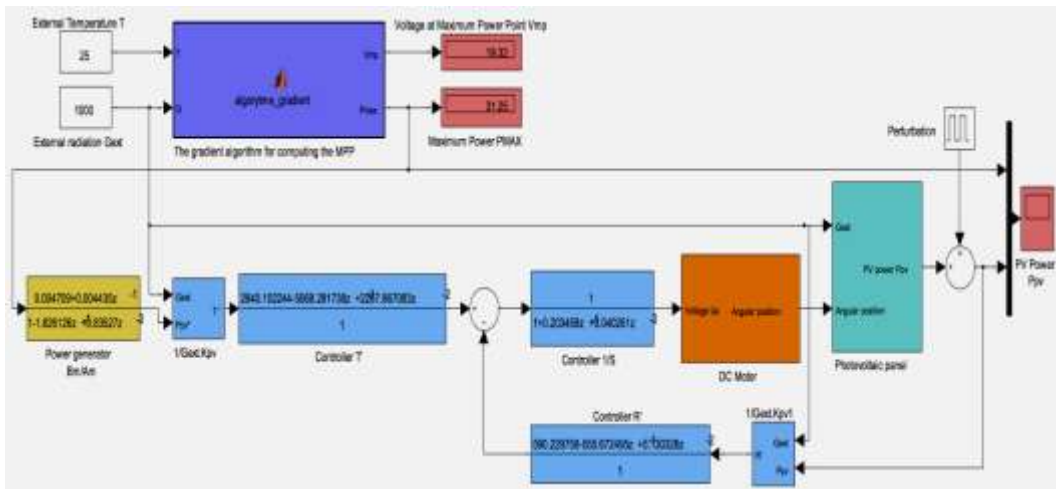
Fig. 8. Simulink diagram of the maximum power point tracking and the control of the motor and the photovoltaic panel by a RST controller.
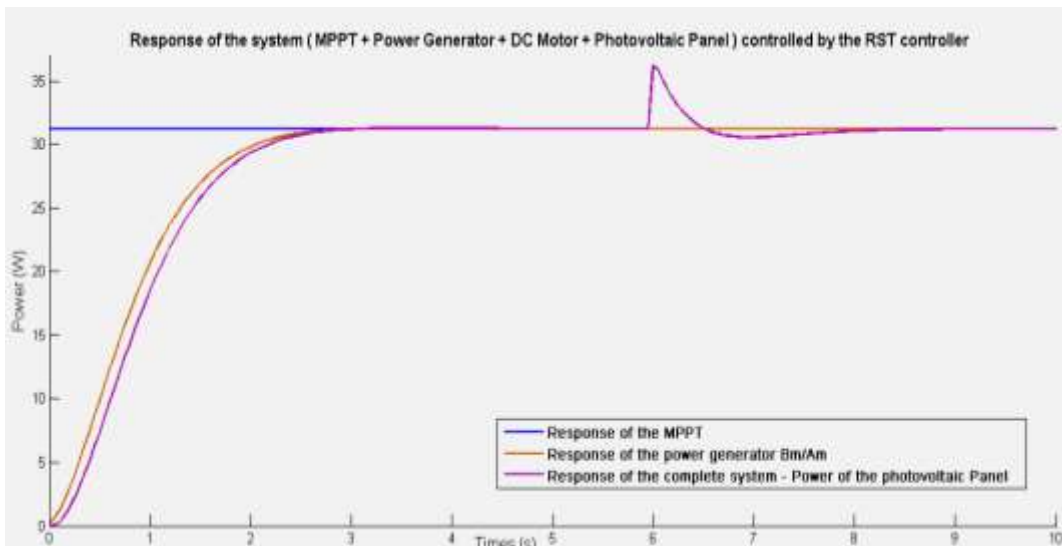

Fig. 9. Response of the system motor and the photovoltaic panel controlled by the RST controller.

4. Maximum power point tracking controlled by a microcontroller Arduino

The objective of this part to implement the previous RST controller in a microcontroller in order to control the system {DC motor + Photovoltaic panel}.

We have used an Arduino Uno, connected to serial port with Simulink.
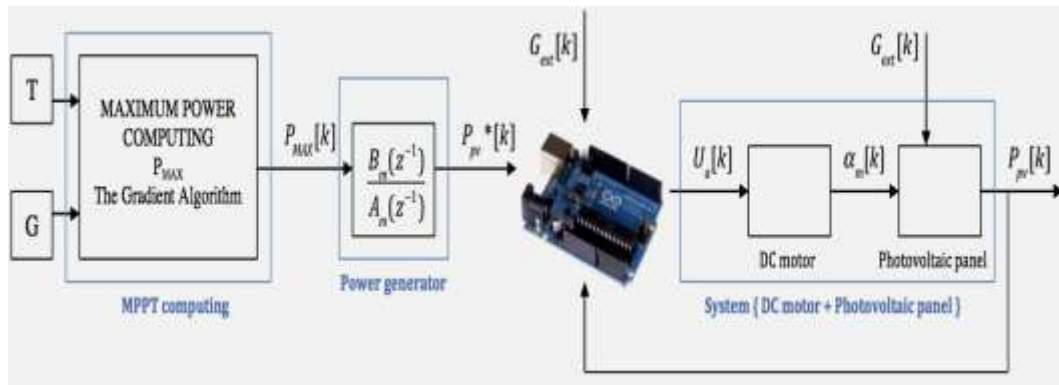
The diagram block becomes:

Fig. 10. Diagram of the maximum power point tracking and control of the system {DC motor + Photovoltaic panel}by an Arduino Uno.

By implement the RST control in the Arduino, we have modified the last Simulink simulation as follows, where the block connected at the Arduino Uno (Packet Output and Packet Input) replaces the blocks concerning the RST controller [9].

The sample time is always of 0.05 seconds.

We have implemented the following formulas in the Arduino:

$$\begin{cases} e[k] = \dfrac{1}{G_{ext}.K_{pv}}\Big(t_0.P_{pv}*[k] + t_1.P_{pv}*[k-1] + t_2.P_{pv}*[k-2] \\ \qquad\qquad - \dfrac{1}{G_{ext}.K_{pv}}\Big(r_0.P_{pv}[k] + r_1.P_{pv}[k-1] + r_2.P_{pv}[k-2]\Big) \\ U_a[k] = e[k] - s_1.U_a[k-1] - s_2.U_a[k-2] \end{cases} \quad (28)$$
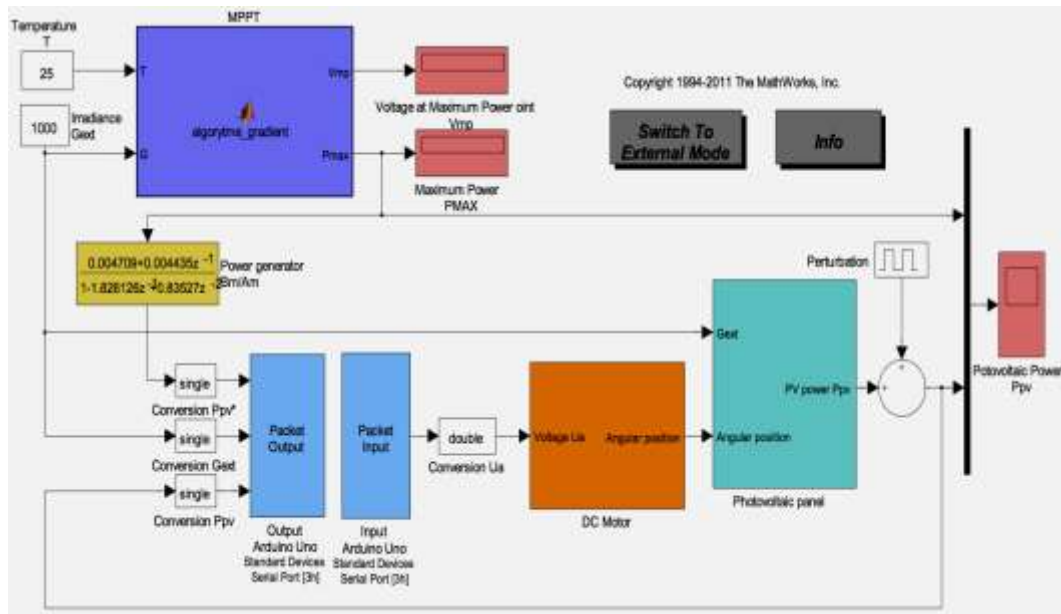
Fig. 11. Simulink diagram of the complete system (MPPT + Power generator + DC Motor + Photovoltaic Panel) controlled by the Arduino Uno

In order to observe the regulation performance, we have inserted a step disturbance at $T = 6$ sec and we can observe that the performances in tracking and in regulation are respected by the system. Furthermore, we can note that there is a delay of 0.5 seconds specific for the Arduino Uno.
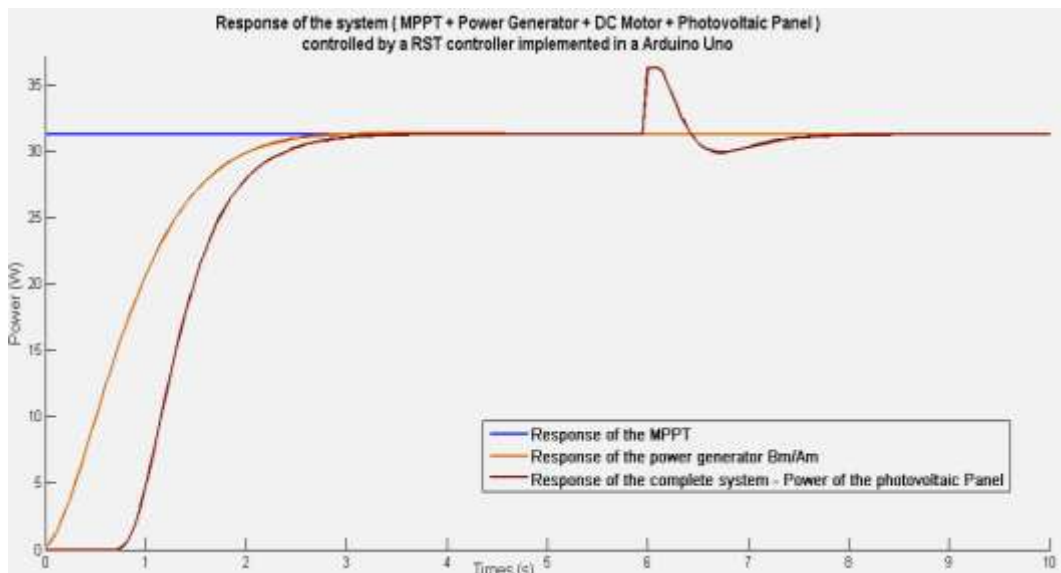

Fig. 12. Results of the Simulink simulation of the complete system (MPPT + Power generator + DC Motor + Photovoltaic Panel) controlled by the Arduino Uno

Conclusions

The paper showed the results obtained in modelling a photovoltaic panel using a two diode model, simulated the panel characteristics and designed a RST controller to position the panel in an optimal position towards the sun.

The gradient algorithm has been shown to obtain the MPP in an optimum number of steps.

The RST controller designed good performance in tracking and regulation and it has been simulated on an Arduino Uno platform.

The HIL (Hardware in the Loop) validation approach can be reiterated for any PV panel and method.

A physical implementation of the system will be made in the near future.

R E F E R E N C E S

[1]   Tarak Salmi, Mounir Bouzguenda, Adel Gastli, Ahmed Masmoudi, MATLAB/Simulink Based Modelling of Solar Photovoltaic Cell, INTERNATIONAL JOURNAL of RENEWABLE ENERGY RESEARCH Tarak Salmi et al., Vol.2, No.2, **2012**.

[2]   Pierre Borne, Dumitru Popescu, Florin Gh, Filip, Dan Ştefănoiu, Optimization in Engineering Sciences Exact Methods, Wiley, **2013**.

[3]   M. Azzouzi, Member, IAENG, L. Mazzouz and D. Popescu Matlab-Simulink of Photovoltaic System Based on a Two-Diode Model, Proceedings of the World Congress on Engineering 2014 Vol I, WCE 2014, July 2 - 4, **2014**, London, U.K.

[4]   Dominique Bonkoungou, Zacharie Koalag, Donatien Njomo, Modelling and Simulation of photovoltaic module considering single-diode equivalent circuit model in MATLAB, International Journal of Emerging Technology and Advanced Engineering Website: www.ijetae.com (ISSN 2250-2459, ISO 9001:2008 Certified Journal, Volume 3, Issue 3, March **2013**).

[5]   Ramos Hernanz, JA.1, Campayo Martín, J.J. Zamora Belver, I., Larrañaga Lesaka, J. Zulueta Guerrero, Modelling of Photovoltaic Module, International Conference on Renewable Energies and Power Quality,(ICREPQ'10),Granada (Spain), 23th to 25th March, **2010**.

[6]   Tiberiu Tudorache1 ,Liviu Kreindler1, Design of a Solar Tracker System for PV Power Plants, Acta Polytechnica Hungarica Vol. 7, No. 1, **2010**.

[7]   I.D. Landau, G. Zito, Digital Control Systems, Springer, **2006**.

[8]   D. Popescu, D. Stefanoiu, C. Lupu, C. Petrescu, B. Ciubotaru, C. Dimon, Automatica Industriala, AGIR, **2006**.

[9]   https://www.arduino.cc/en/Guide/HomePage.